university of groningen

University Medical Center Groningen

University of Groningen

Coherent control of electron spin dynamics in nano-engineered semiconductor structures

Denega, Sergii Zinoviyovych

IMPORTANT NOTE: You are advised to consult the publisher's version (publisher's PDF) if you wish to cite from it. Please check the document version below.

Document Version
Publisher's PDF, also known as Version of record

Publication date:
2011

Link to publication in University of Groningen/UMCG research database

Citation for published version (APA):
Denega, S. Z. (2011). *Coherent control of electron spin dynamics in nano-engineered semiconductor structures*. s.n.

Copyright
Other than for strictly personal use, it is not permitted to download or to forward/distribute the text or part of it without the consent of the author(s) and/or copyright holder(s), unless the work is under an open content license (like Creative Commons).

Take-down policy
If you believe that this document breaches copyright please contact us providing details, and we will remove access to the work immediately and investigate your claim.

Downloaded from the University of Groningen/UMCG research database (Pure): http://www.rug.nl/research/portal. For technical reasons the number of authors shown on this cover page is limited to 10 maximum.

Download date: 23-09-2021

Chapter 7

Optical time-resolved study of the Landé g factor in n-doped GaAs materials

Abstract

We present time- and energy-resolved measurements of the electron g factor in GaAs materials with Si donors at concentrations at and below the metal-insulator transition ($n \approx 10^{13}$ to 2×10^{16} cm^{-3}). Results were obtained with optical Kerr readout. We studied the dependence on doping concentration, density of photo-carriers, photon energies and magnetic field. While the widely reported g factor values for these conditions predict $g \geqq -0.44$, we systematically find values in the range -0.49 to -0.44 for delocalized electrons at low energies in samples where donor sites form a band. With a wavelet analysis a drift of g factor values during transient spin precession signals is revealed. The spin dynamics in this regime provides a test for fundamental understanding of semiconductors, and complete characterization is a prerequisite for optical studies of GaAs-based spintronic devices.

7.1 Introduction

The Landé g factor for an electronic state in a semiconductor is highly sensitive to the associated band structure. Detailed studies of g factor values therefore provide an interesting test for our fundamental understanding and theoretical modeling of these materials [1, 2, 3, 4, 5]. Semiconductor materials are also central in research that aims to develop spintronic functionalities. Here, knowing g factor values is essential, and it is of interest to understand how material parameters influence the g factor values. A distribution of g factor values within a precessing electron spin ensemble can dominate the inhomogeneous loss of spin coherence, and it is interesting to understand how external control on a device can manipulate the g factor [6].

For direct band-gap semiconductors, optical time-resolved Kerr-rotation (TRKR, as used in this work) and Faraday-rotation measurements have been established as standard techniques for the characterization of electron spin dynamics [7]. By tuning the experimental parameters such as photon energy, external magnetic field, and intensity of the optical pump beam one can study the response in different materials, including complex layered structures [8, 9, 10, 11, 12, 13]. This points to another situation that requires reliable knowledge about g factors: When the TRKR technique is applied to studies of spin dynamics in GaAs/AlGaAs and GaAs/InGaAs heterostructures, TRKR signals can be a superposition of signal contributions from different layers, which can be unraveled using differences in g factor [14, 11, 12]. Such studies also require knowledge about the instantaneous g factor value during intraband kinetic energy relaxation of photo-electrons.

We report here a time- and energy-resolved study of the electron g factor in GaAs materials with Si donor concentrations n at and below the metal-insulator transition (MIT), using samples with $n \approx 10^{13}$ to 2×10^{16} cm^{-3}. GaAs materials with this MIT level of doping ($n \approx 2 \times 10^{16}$ cm^{-3}) were extensively studied in recent years, since the spin dephasing time as a function of n peaks here at an exponentially enhanced value [15, 16, 17]. Despite this large body of earlier work, we found in our studies on this material g factor values that strongly deviate ($-0.49 < g < -0.44$) from what is commonly reported ($g \gtrapprox -0.44$) for MIT materials, or even any GaAs material. We carried out TRKR studies at very low optical intensities and with low photon energies and find that g factors $g < -0.44$ originate from delocalized electrons in the donor band. We support this conclusion by studying in parallel ultrapure GaAs samples without a donor

band, but which still have a very low level of intentional doping with Si donors. This allowed us to confirm that the g factors $g < -0.44$ do not occur for localized donor-bound electrons (D^0 systems, which have $g \approx -0.42$) or for free electrons in the intrinsic conduction band. Thus, our work includes TRKR studies that directly probe the spin dynamics of such D^0 systems. Previously used techniques were not sensitive to D^0 spins [16], or could not distinguish between the contribution from conduction electrons and these donor-bound electrons [18, 5, 19, 20].

The most widely reported value for the GaAs g factor is $g = -0.44$. In addition, it is well described that $g > -0.44$ can occur due to a diamagnetic shift of the electronic levels, band filling, and quantum confinement in a GaAs layer. This behavior can be approximated as

$$g = g_0 + \gamma E, \tag{7.1}$$

where E is the electron kinetic energy E (with respect to the bottom of the conduction band). The accepted values for bulk GaAs are [1, 21, 22] $g_0 \approx -0.44$ and $\gamma \approx 6.3$ eV^{-1}. There were, nevertheless, a few reports that mentioned g factors $g < -0.44$ without making a systematic study of this deviation [23]. Only recently, Hübner *et al.* [5] reported for the first time a systematic study with g factors in the range -0.49 to -0.44 for low-energy electrons in a GaAs sample with 1.2×10^{15} cm^{-3} Si doping. These authors suspected these values could be only observed with their low-invasive measurement technique (spin-quantum-beat spectroscopy of photoluminescence signals). We extend this study here by applying TRKR as a fully time- and energy-resolved measurement technique, and by including a wider range of doping concentrations. Our work demonstrates that the g factors in the range -0.49 to -0.44 can also be observed and studied with TRKR. However, while the authors of Ref. [5] conclude that the g factors $g < -0.44$ occur for low-energy electrons in the intrinsic conduction band (rather than delocalized electrons at donor levels), our work points to the opposite conclusion.

We strengthen our analysis by applying a wavelet transform for directly analyzing the role of drifting g factor values during transient TRKR signals. This allows for getting fully time-resolved measurements of the g factor for optically induced spin coherence. The results are consistent with the picture that g factors get closer to zero with increasing kinetic energy for electron populations in bands.

7.2 Results

For our experiments we used three GaAs samples with Si doping at different concentrations: sample A and B have donor concentrations 3×10^{13} cm^{-3} and 1×10^{14} cm^{-3}, respectively (the same materials as in Refs. [24, 25], without epitaxial lift-off). At these low concentrations the donor electrons are localized around the Si sites and neighboring electrons do not interact. Sample C is the MIT sample with $n \approx 2 \times 10^{16}$ cm^{-3} (the same wafer material as in Ref. [26]), in which the donor states form a band. All experiments were performed at a temperature of 4.2 K in an optical cryostat with a superconducting magnet for supplying fields up to 7 T. The applied fields at the sample location were known with a precision better than 1 part in 10^3. For the TRKR measurements we used the Voigt geometry (light propagation perpendicular to the sample plane, while the external magnetic field is in plane of the sample).

A tunable Ti:sapphire laser with ∼150 fs pulses at 80 MHz repetition rate provided the pump and probe beams for the TRKR technique. The beams were focused into fully overlapping spots on the sample with a diameter of 120 μm. The spectrum of pulses was narrowed down to $\Delta\lambda = 1.2$ nm by tunable Fabry-Pérot filters. This allowed us to have better energy selectivity while keeping the time resolution in the experiment below 1 ps. Both pump and probe were filtered separately, which gave the possibility to perform single- (pump and probe beam at the same wavelength) and two-color (pump and probe beam at different wavelengths) TRKR experiments with a single laser source. The polarization of the pump pulses was modulated between σ^+ and σ^- with a photoelastic modulator at 50 kHz. This ensures that dynamical nuclear polarization effects are negligible in our experiments. While varying the time delay t between pump and probe pulses the rotation of the reflected probe pulse was recorded. A typical TRKR trace is presented in Fig. 7.1(a).

Figure 7.1(b) presents photoluminescence (PL) data from samples A, B and C. The relative peak strength of the donor-bound exciton emission (labeled D^0X) gets more pronounced with increasing doping concentration, while the contribution from free excitons (X) gets weaker. Mapping out these PL spectra for all magnetic fields is important for proper selection of the pump and probe photon energies in our TRKR experiments (but for sample C we will also use the spectral dependence of the TRKR signals themselves, as discussed later). Unless stated otherwise, our TRKR studies focused on resonant probing of electrons in the energetically lowest states that appeared in the PL spectra. In sample A and B

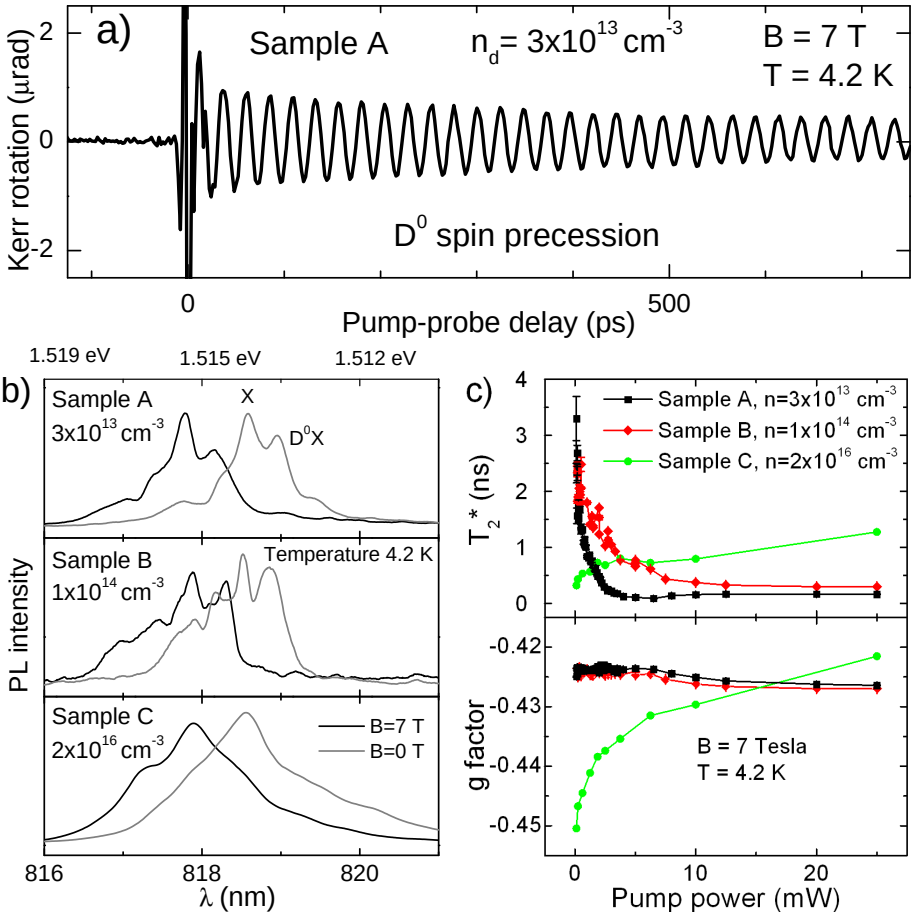

Figure 7.1: (a) Typical example of a TRKR signal from D^0 spins in sample A (single-color TRKR with $\lambda = 818.5$ nm and 1 mW pump power). (b) Photoluminescence results from samples A, B and C for $B = 0$ T (gray) and $B = 7$ T (black) (the narrowest spectral features correspond to the resolution of the spectrometer). (c) Spin dephasing time (T_2^*) and g factors as a function of the pump beam power. The pump and probe wavelengths used in this study were tuned at the donor photoluminescence peak for all three samples.

this concerns the optical transition between the localized D^0 system and the localized donor-bound exciton complex (D^0X system). However, for sample C the PL peak can not simply be attributed to donor levels. At donor concentrations $n \approx 10^{15}$ cm^{-3} the wave functions of neighboring donor electrons already overlap for a significant portion of the donors. With increasing n this further develops into a donor band that touches the intrinsic GaAs conduction band. This means that the low-energy PL emission comes from the recombination of delocalized

excitons.

A consequence of the above is that the spin dephasing times T_2^* and g factors (as derived from TRKR traces) differ qualitatively for samples with doping below (A and B) and above (C) the donor-band formation point in their dependence on experimental parameters. Figure 7.1(c) shows clearly different behavior for the dependence of T_2^* and g on the optical pump power for n-doping above and below of 10^{15} cm^{-3}. Notably, for sample A and B at low pump powers these TRKR results reflect spin precession of D^0 electrons (here preparation and detection occurs via a stimulated Raman process, and the carriers in the D^0X complex do not contribute to the signal [25]). These show a constant g factor of $g = 0.423$ (at $B = 7$ T) up to pumping with 7 mW. For stronger pumping sample A and B show very short-lived TRKR signals that also start to reflect spin precession of delocalized electrons (with $g \approx -0.44$), since the excitation of free excitons is no longer negligible. A detailed discussion of this data from sample A and B is presented in Ref. [27].

Sample C, on the other hand, shows a g factor that sharply increases from $g = -0.45$ (at $B = 7$ T). For such a MIT sample it is difficult to draw a clear line between the donor band and the conduction band. Band filling effects are here responsible for the continuous dependence of the g factor on pump power. At low pump power the measured g factor represents the value that corresponds to the electronic levels that are in resonance with the probe photon energy. At higher pump powers, the dependence of g on pump power is due to the rise of the quasi-Fermi level for photo-electrons, and it thereby reflects the dependence of the g factor on energy (Eq. (7.1), the energies of the states that dominate the TRKR response increase due to the band filling [22]). The increase of T_2^* with pump power for sample C is consistent with the theory for spin dephasing in the metal-insulator transition phase [16].

We further explored the sharp decrease in g to values below $g = -0.44$, as observed with sample C while going to very low pump powers [Fig. 7.1(c)]. Our further studies concentrate on behavior in a weaker magnetic field of $B =$ 1 T. Here, the g factors have less of a diamagnetic shift towards zero, while the precession frequency is still high enough for precise measurements of g. Since it is for sample C difficult to distinguish between conduction- and donor-band electrons, we first made a detailed TRKR study at low pump powers, with the pump photon energy above the band gap and for different probe photon energies (Fig. 7.2). With the narrow spectral width of the probe beam ($\Delta\lambda \approx 1.2\ nm$) we thus get TRKR traces for which the response is dominated by electrons from

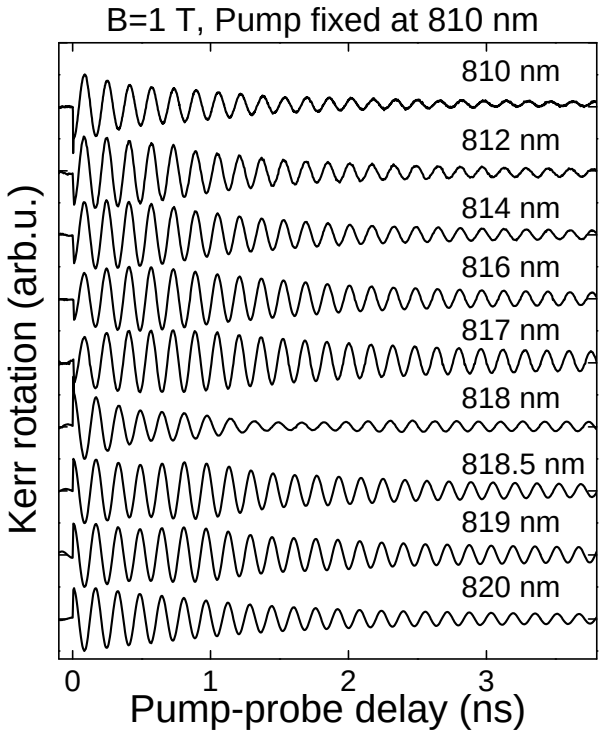

Figure 7.2: TRKR signals from Sample C, showing the dependence on probe photon energy (labeled as wavelengths). For all traces pumping occurred with 810 nm light at 1 mW. Probing with light around 818 nm shows TRKR traces with non-monotonous behavior of the envelop function, and this marks the transition from donor-band to conduction-band dominated response.

either the donor-band states or the conduction-band states. For $B = 1$ T the expected energy for the intrinsic band gap corresponds to ∼818 nm probe light [28]. We observe indeed a clear transition around 817.5 nm in the series of TRKR traces in Fig. 7.2, as summarized in these points:

(1) There is a sign flip for the Kerr rotation (consistent with a sign flip for the spin-selective dispersion [29]), associated with a switch from blue-detuned to red-detuned probing of a resonance.

(2) In particular the trace for 818 nm shows that the TRKR can be sensitive to conduction and donor electrons at the same time, possibly also influenced by relaxation dynamics between these two populations. This signal shows a node in its envelope around 1.8 ns delay, and an overall reduction in amplitude. Similar effects were observed in recent transmission experiments [30, 31].

(3) Traces with probe photon energies higher than the band gap have a signal

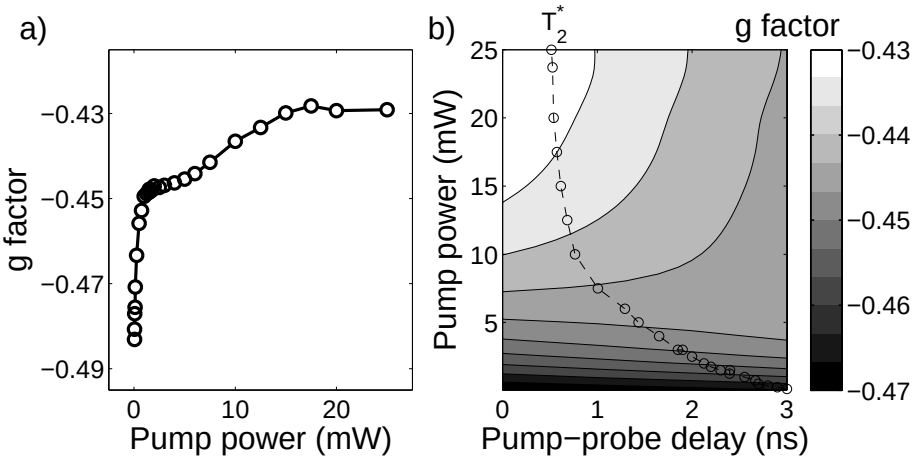

Figure 7.3: Values of the g factor from TRKR signals from sample C. (a) Dependence on pump beam intensity. Here g factors are determined from a Fourier transform of TRKR data. Pump and probe were at 819 nm and $B = 1$ T. (b) Dependence of g factor values (gray scale) on pump beam intensity and pump-probe delay. Here g factors are derived with a wavelet analysis (see main text). The dashed line indicates the spin dephasing time T_2^* for the TRKR trace at a particular pump power.

envelope that shows a slow growth during the first few hundred picoseconds due to carrier cooling (intraband relaxation) [30].
(4) Traces with probe photon energies smaller than the band gap show longer T_2^* values. This is most clearly observed as a residual spin precession signal at negative delays (spin memory effect [15]) that occurs when $T_2^* \gtrapprox T_{rep} = 12.5$ ns (the repetition time for the laser).

We conclude from the study in Fig. 7.2 that for $B = 1$ T probing with wavelengths $\lambda_p \geqq 819$ nm gives at low pump powers TRKR signals that predominantly represent spin precession of electrons in the donor band. Figure 7.3(a) presents for these conditions and $\lambda_p = 819$ nm the g factor values as a function of pump power. Here g factors decrease to well below -0.48 for the lowest pump powers that we could use. These g factors were derived from the peak in Fourier transforms of TRKR traces, that show a single narrow peak for the lowest pump powers. However, the data in Fig. 7.2 shows that several of the TRKR traces are clearly sensitive to the interplay between different electron levels and relaxation. This could also manifest itself as drifting g factors during the TRKR traces. We therefore also carried out a wavelet analysis on the data that underlies Fig. 7.3(a), which can make any relaxation process that influences the observed g factor directly visible.

The continuous wavelet transform allows to extract instantaneous oscillation frequencies in a signal [32, 33]. Guided by these references, we choose the Morlet wavelet for our analysis to obtain the frequency f that is most strongly present in the TRKR signal around delay t', and then convert to a g factor with $g = hf/\mu_B B$. The wavelet transform of a TRKR signal $\Theta_k(t)$ is

$$W_\Theta(f, t') = \int_0^\infty \Theta_k(t) \cdot M(t') \cdot dt, \tag{7.2}$$

where $M(t')$

$$M(t') = \frac{1}{\sqrt{\pi \Delta t^2}} \cdot e^{-2\pi i f t} \cdot e^{-\frac{(t-t')^2}{\Delta t^2}} \tag{7.3}$$

is the Morlet wavelet. The parameter Δt controls here the trade-off between resolution in time and frequency. We analyzed that $\Delta t = 250$ ps is a suitable value for our analysis. For this particular wavelet the analysis is equivalent to a sliding-window Fourier transform. Figure 7.3(b) present results of applying this procedure to the data that underlies Fig. 7.3(a). The gray scale represents the extracted g factor as a function of pump power and delay t. The spin dephasing time for each pump power is indicated on the plot with a dashed line (estimate based on fitting TRKR oscillations with a mono-exponentially decaying envelope). The plot confirms that intraband relaxation processes influence the instantaneous g factor values.

For the very lowest pump powers in Fig. 7.3(b), the g factor is nearly constant at $g \approx -0.48$, while the spin dephasing time grows to a value above 3 ns (unlike the data in Fig. 7.1(c) where the high-field causes rapid precessional dephasing due to a small spread in g-factors). This suggests that the values $g \lessapprox -0.48$ are for electrons in the donor band in the limit of zero pump intensity and low field. For the results with pump powers between ∼1 mW and ∼6 mW there is a small increase in the g factor values during the first 3 ns. For example, the trace for 3 mW shows an increase from $g \approx -0.455$ to $g \approx -0.445$. This behavior is at this stage not fully understood. At the highest pump powers the drift in g factor values is clearly pointed towards more negative values. Here the density of photoelectrons is much higher than the electron density due to doping, such that the Kerr signal decays over a timescale that is close to the electron-hole recombination time. During this process the quasi-Fermi level goes down, and along with this the g factor (as for Eq. 7.1). Initially, the donor band is here completely occupied. Therefore, most of the Kerr rotation signal is then coming from conduction band electrons. The values $g \gtrapprox -0.44$ corresponds to the conduction band electrons (which is consistent with most of the earlier observations [1, 26]).

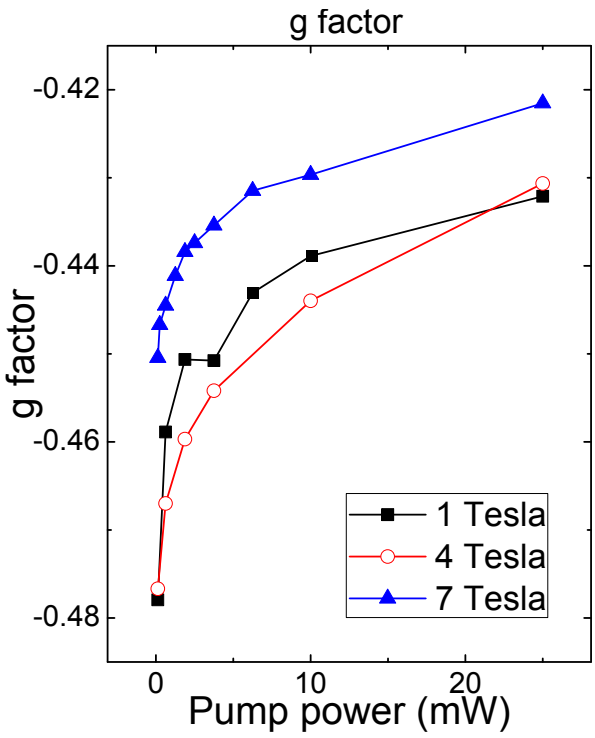

Figure 7.4: Values of the g factor from TRKR signals from sample C, as a function of pump beam intensity at different values for magnetic field. For this data set the probe-wavelength was *not* adjusted for the diamagnetic shift of the band gap energy.

The presented measurements on sample C thus indicate that the values $-0.49 < g < -0.44$ originate from electrons in the donor band. We used TRKR studies on sample A and B for a test of this hypothesis. In particular, these sample are ultra pure with a low level of n-doping. This gives an ensemble of D^0 systems that can be addressed with TRKR while not addressing electrons in the intrinsic conduction band at the same time [25]. With these samples we can thus test whether $g \approx -0.48$ can also be observed on localized D^0 systems, or free excitons in a very pure material. Our studies to this end only showed $g \approx -0.423$ for the D^0 systems (see Fig. 7.1(c)), while low pump-power studies near resonance with the free exciton transition only showed $g \approx -0.44$. Thus, we conclude that g factors values $-0.49 < g < -0.44$ only occur for *delocalized* electrons in donor-band states.

Our data does illustrate why the g factor and T_2^* values that were reported by the field till now showed such large variation, while g factors $g < -0.44$ were almost never reported. Different measurement techniques reported values that

differed more than the reported measurements error [1, 2, 30, 34, 35, 5]. The discrepancy is often hidden in the techniques themselves, meaning that different levels of background doping in samples, photo-excitation power and excitation/detection photon energies result in different results. The measured g factor value is a function of the experimental parameters, and this restricts the relevance of the reported value.

The data in Fig. 7.3(a) represent a clear example. It shows that the g-factor value as a function of optical pumping intensity seems to saturate at a value of about $g = -0.445$ when going to lower pump powers. Only pumping with very low powers (below 1 mW) reveals the sudden trend towards $g = -0.49$, and is thus easily overlooked. Another example is the dependence on probe wavelength in Fig. 7.2, which can in a similar manner hamper a study as a function of magnetic field. This is the case for the data set that we present in Fig. 7.4. This plot present g factors from TRKR traces recorded at different values of the external magnetic field and pump power (single-color TRKR experiments). Here the probe wavelength was *not* adjusted for the small diamagnetic shift of the band gap. This yields a non-monotonous dependence of g factors on B, which is hard to interpret without further studies.

7.3 Conclusions

In conclusion, we applied the TRKR technique to n-doped GaAs materials with different doping concentrations. We reproduced the recently reported unconventional g factor values [5] ($-0.49 < g < -0.44$). Our studies indicate that these g-factor values originate from delocalized electrons in donor-band states, while localized donor electrons exhibit $g \approx -0.42$. Furthermore, our study yields the value $g \approx -0.44$ for electrons at the bottom of the intrinsic conduction band of GaAs.

We obtained these results by applying the conventional TRKR technique with optimized time- and energy resolution. For our results it was crucial to have the ability to work at weak optical power levels, which we obtained after technical improvements to our detection scheme. We thus showed that the TRKR technique can be applied with about 2 meV energy resolution and at very low optical intensities, such that it is suited for separately studying the spin dynamics of donor electrons and conduction band electrons in samples with very low doping levels. We also extended the standard time-resolved Kerr rotation investigations with a wavelet analysis and this gives access to time-resolved information about

g factor values. The technique can be further extended with the recently reported method for determining the sign of a g factor from TRKR measurements [36]. TRKR is therefore highly suited for the characterization of the response from substrates or host materials with fully controlled experimental conditions, before analyzing the data from more complex structures [10, 11, 12]. Still, the method should be applied with care since even in a single GaAs layer inter- and intraband relaxation processes can lead to non-trivial TRKR traces (Ref. [30], and Fig. 7.2).

We thank M. Sladkov, B. Wolfs, F. Pei, B. Visser and A. Rudavskyi for help and stimulating discussions, and are grateful for financial support from the Dutch NWO and NanoNed, and the German programs BMBF nanoQUIT, Research school Ruhr-Universität Bochum, DFG-SFB 491 and DFG-SPP 1285.

References

[1] C. Weisbuch, and C. Hermann, Phys. Rev. B **15**, 816-822 (1977).

[2] M. Oestreich, and W. W. Rühle, Phys. Rev. Lett. **74**, 2315 (1995).

[3] R. Winkler, *Spin-Orbit Coupling Effects in Two-Dimensional Electron and Hole Systems* (Springer, 2003).

[4] K. Shen, M. Q. Weng, and M. W. Wu, Journal of Applied Physics **104**, 063719 (2008).

[5] J. Hübner, S. Döhrmann, D. Hägele, and M. Oestreich, Phys. Rev. B **79**, 193307 (2009).

[6] L. Meier, G. Salis, I. Shorubalko, E. Gini, S. Schon, and K. Ensslin, Nature Phys. **3**, 650 (2007).

[7] D. Awschalom and N. Samarth, Physics **2** (2009), ISSN 1943-2879.

[8] I. A. Yugova, A. Greilich, D. R. Yakovlev, A. A. Kiselev, M. Bayer, V. V. Petrov, Yu. K. Dolgikh, D. Reuter, and A. D. Wieck, Phys. Rev. B **75**, 245302 (2007).

[9] N. Porrasmonenegro, C. Perdomoleiva, E. Reyesgomez, H. Brandi, and L. Oliveira, Microelectronics Journal **39**, 390 (2008), ISSN 00262692.

[10] H. Luo, X. Qian, X. Ruan, Y. Ji, and V. Umansky, Physical Review B **80**, 2 (2009), ISSN 1098-0121.

[11] P. J. Rizo, A. Pugzlys, A. Slachter, S. Z. Denega, D. Reuter, A. D. Wieck, P. H. M. van Loosdrecht and C. H. van der Wal, New J. Phys. **12** 113040 (2010).

[12] S. Z. Denega, T. Last, J. Liu, A. Slachter, P. J. Rizo, P. H. M. van Loosdrecht, B. J. van Wees, D. Reuter, A. D. Wieck, C. H. van der Wal, Phys. Rev. B **81**, 153302 (2010).

[13] L. V. Fokina, I. A. Yugova, D. R. Yakovlev, M. M. Glazov, I. A. Akimov, A. Greilich, D. Reuter, A. D. Wieck, and M. Bayer, Phys. Rev. B **81**, 195304 (2010).

[14] I. Malajovich, J. M. Kikkawa, D. D. Awschalom, J. J. Berry, and N. Samarth, Phys. Rev. Lett. **84**, 1015 (2000).

[15] J.M. Kikkawa, and D. D. Awschalom, Phys. Rev. Lett. **80**, 4313 (1998).

[16] R. I. Dzhioev, K. V. Kavokin1, V. L. Korenev, M. V. Lazarev, B. Ya. Meltser, M. N. Stepanova, B. P. Zakharchenya, D. Gammon, and D. S. Katzer, Phys. Rev. B **66**, 245204 (2002).

[17] M. Römer, H. Bernien, G. Müller, D. Schuh, J. Hübner1, and M. Oestreich, Phys. Rev. B **81**, 075216 (2010).

[18] M. Oestreich, M. Römer, R. J. Haug, and D. Hägele, Phys. Rev. Lett. **95**, 216603 (2005).

[19] S. A. Crooker, L. Cheng, and D. L. Smith, Phys. Rev. B **79**, 035208 (2009).

[20] G. M. Müller, M. Römer, J. Hübner, and M. Oestreich, Phys. Rev. B **81**, 121202(R) (2010).

[21] W. Zawadzki, and P. Boguslawski, Phys. Rev. Lett. **31** 1403 (1973).

[22] M. J. Yang, R. J. Wagner, B. V. Shanabrook, J. R. Waterman, and W. J. Moore, Phys. Rev. B **47**, 6807 (1993).

[23] M. Krapf, H. Pascher, G. Weimann, and W. Schlapp, Solid State Commun. **78**, 459 (1991).

[24] M. Sladkov, A. U. Chaubal, M. P Bakker, A. R. Onur, D. Reuter, A. D. Wieck, and C. H. van der Wal, Phys. Rev. B **82**, 121308(R) (2010).

[25] S. Z. Denega, M. Sladkov, D. Reuter, A. D. Wieck, T. L. C. Jansen, C. H. van der Wal, arXiv:1103.4307 (2011).

[26] P. E. Hohage, G. Bacher, D. Reuter, and A. D. Wieck, Appl. Phys. Lett. **89**, 231101 (2006).

[27] M. Sladkov, PhD thesis (Univeristy of Groningen, 2011).

[28] L. Viña, S. Logothetidis, and M. Cardona, Phys. Rev. B **30**, 1979 (1984).

[29] A. V. Kimel, F. Bentivegna, V. N. Gridnev, V. V. Pavlov, and R. V. Pisarev, and Th. Rasing, Phys. Rev. B **63**, 235201 (2001).

[30] L. Schreiber, M. Heidkamp, T. Rohleder, B. Beschoten, G. Güntherodt, arXiv:0706.1884 (2007).

[31] T. Lai, L. Teng, Z. Jiao, H. Xu, L. Lei, J. Wen, and W. Lin, Appl. Phys. Lett. **91**, 062110 (2007)

[32] N. Delprat, B. Escudie, P. Guillemain, R. Kronland-Martinet, P. Tchamitchian, and B. Torresani, IEEE Transactions on Information Theory **38**, 644 (1992).

[33] E. L. Schukin, R. Zamaraev, and L. Schukin, Mechanical Systems and Signal Processing **18**, 1315 (2004).

[34] W. Zawadzki, P. Pfeffer, R. Bratschitsch, Z. Chen, S. Cundiff, B. Murdin, and C. Pidgeon, Physical Review B **78**, 1 (2008).

[35] K. Litvinenko, L. Nikzad, C. Pidgeon, J. Allam, L. Cohen, T. Ashley, M. Emeny, W. Zawadzki, and B. Murdin, Physical Review B **77**, 2 (2008).

[36] C. L. Yang, J. Dai, W. K. Ge, and X. Cui, Applied Physics Letters **96**, 152109 (2010).